Cancer Cell
Article

Tumor Stroma-Derived TGF-β Limits Myc-Driven Lymphomagenesis via Suv39h1-Dependent Senescence

Maurice Reimann,[1,6] Soyoung Lee,[1,2,6] Christoph Loddenkemper,[3,6,7] Jan R. Dörr,[1,6] Vedrana Tabor,[2,6] Peter Aichele,[4] Harald Stein,[3] Bernd Dörken,[1,2] Thomas Jenuwein,[5,8] and Clemens A. Schmitt[1,2,*]
[1]Charité - Universitätsmedizin Berlin/Molekulares Krebsforschungszentrum der Charité - MKFZ, 13353 Berlin, Germany
[2]Max-Delbrück-Center for Molecular Medicine, 13125 Berlin, Germany
[3]Charité - Universitätsmedizin Berlin/Department of Pathology, Campus Benjamin Franklin, 12200 Berlin, Germany
[4]Department of Immunology, University Hospital Freiburg, 79104 Freiburg, Germany
[5]Research Institute of Molecular Pathology, 1030 Vienna, Austria
[6]These authors contributed equally to this work
[7]Present address: Technische Universität München, Institute of Pathology, 81675 Munich, Germany
[8]Present address: Max-Planck-Institute of Immunology, 79108 Freiburg, Germany
*Correspondence: clemens.schmitt@charite.de
DOI 10.1016/j.ccr.2009.12.043

SUMMARY

Activated RAS/BRAF oncogenes induce cellular senescence as a tumor-suppressive barrier in early cancer development, at least in part, via an oncogene-evoked DNA damage response (DDR). In contrast, Myc activation—although producing a DDR as well—is known to primarily elicit an apoptotic countermeasure. Using the Eμ-*myc* transgenic mouse lymphoma model, we show here in vivo that apoptotic lymphoma cells activate macrophages to secrete transforming growth factor β (TGF-β) as a critical non-cell-autonomous inducer of cellular senescence. Accordingly, neutralization of TGF-β action, like genetic inactivation of the senescence-related histone methyltransferase Suv39h1, significantly accelerates Myc-driven tumor development via cancellation of cellular senescence. These findings, recapitulated in human aggressive B cell lymphomas, demonstrate that tumor-prompted stroma-derived signals may limit tumorigenesis by feedback senescence induction.

INTRODUCTION

Mitogenic oncogenes provoke checkpoint-mediated cellular countermeasures such as apoptosis or premature senescence, a terminal G1 arrest involving the p53 and $p16^{INK4a}$ tumor suppressors that is characterized by typical transcriptional, biochemical and morphological alterations (Campisi and d'Adda di Fagagna, 2007; Hemann and Narita, 2007). RAS- or BRAF-initiated senescent lesions in vitro and in vivo exhibit chromatin changes that include the transcriptionally repressive trimethylation mark at H3K9 (H3K9me3) and focal enrichment of HP1 proteins for which H3K9me3 provides a docking site (Bartkova et al., 2006; Braig et al., 2005; Collado et al., 2005; Lachner et al., 2001; Michaloglou et al., 2005; Narita et al., 2003). Mechanistically, hypophosphorylated retinoblastoma (Rb) protein, bound to growth-promoting E2F transcription factors, may recruit H3K9 methyltransferase activities such as Suv39h1 to direct heterochromatinization to the vicinity of E2F-responsive promoters, thus silencing S-phase genes (Narita et al., 2003). Increasing evidence points towards an oncogene-induced DDR as critical upstream trigger of the senescence program (Bartkova et al., 2006; Di Micco et al., 2006; Mallette

Significance

Cancer entities with constitutive Myc expression, among them aggressive B cell lymphomas, typically display high levels of apoptosis. So far, cellular senescence as another oncogene-inducible safeguard program has been recognized in RAS/BRAF-driven scenarios, but not as a bona fide Myc-evoked anticancer mechanism. Utilizing the genetically tractable Eμ-*myc* transgenic mouse lymphoma model and presenting supportive evidence from human aggressive B cell lymphoma samples, this study establishes a network of tumor/host immune cell interactions in which apoptotic tumor cells launch a paracrine response in non-malignant bystanders that limits lymphomagenesis by cellular senescence. Our data expand the relevance of oncogene-induced senescence to Myc-driven cancers, and highlight the tumor stroma as a critical contributor and potential therapeutic target in this process.

et al., 2007). Indeed, Myc and RAS oncogenes cause DNA damage by inducing reactive oxygen species (ROS) and generating stalled DNA replication intermediates (Di Micco et al., 2006; Lee et al., 1999; Reimann et al., 2007; Vafa et al., 2002). However, both prototypic oncogenes produce very different outcomes—i.e., predominantly cellular senescence following RAS/BRAF and apoptosis in response to Myc activation—when activated in primary cells in vitro (Evan et al., 1992; Serrano et al., 1997).

So far, there has been no clear evidence that Myc induction in primary cells may cause senescence under physiological conditions in vitro or in vivo (Feldser and Greider, 2007; Grandori et al., 2003; Guney et al., 2006). One cell-autonomous explanation for Myc's primarily proapoptotic action might be that Myc favors apoptosis over arrest by influencing p53-dependent transactivation processes in response to DNA damage (Seoane et al., 2002).

The purpose of this study was to determine the contribution of cellular senescence as a tumor-suppressive mechanism in a transgenic mouse model of Myc-driven lymphomagenesis reminiscent of aggressive B cell lymphomas in humans. Given the well-established predominantly apoptotic response to Myc activation in primary cells in vitro, we specifically aimed to dissect cell-autonomous and non-cell-autonomous components of Myc-related senescence in vivo.

RESULTS

Suv39h1-Dependent Cellular Senescence Limits Myc-Induced Lymphomagenesis

To determine the role of cellular senescence in Myc-driven tumorigenesis, we studied the impact of senescence-compromising Suv39h1 loss in Eμ-*myc* transgenic mice (Adams et al., 1985; Braig et al., 2005), where genetic disruption of apoptosis strongly promotes B cell lymphomagenesis (Egle et al., 2004; Schmitt et al., 2002b; Strasser et al., 1990). Mice that lacked one or both *Suv39h1* alleles developed lymphomas significantly faster than mice without a targeted defect at the *Suv39h1* locus ($p < 0.0001$ for either comparison, Figure 1A). Moreover, lymphomas that formed in *Suv39h1*$^{+/-}$ female mice invariably lost expression of the X-chromosomally encoded *Suv39h1* transcript, thereby explaining the indistinguishable tumor onset in *Suv39h1*$^{+/-}$ and *Suv39h1*$^{-}$ (i.e., *Suv39h1*$^{-/y}$ male and *Suv39h1*$^{-/-}$ female) mice (Figure 1A, insert). Importantly, the frequency of apoptosis measured as TUNEL reactivity, a hallmark of Myc-driven lymphomas, was virtually identical in Suv39h1-deficient lymphomas when compared to control lymphomas (i.e., those that arose in Eμ-*myc* mice without a targeted *Suv39h1* lesion; Figure 1B). Furthermore, control and Suv39h1-deficient lymphomas presented with indistinguishable gross pathology, formed at comparable stages of B cell development, both expressed *Suv39h2* transcripts, and displayed similar near-normal chromosome counts, unlike the previously reported chromosome-missegregated B cell lymphomas that form in the absence of both *Suv39h1* and *Suv39h2* alleles in nontransgenic mice (Peters et al., 2001) (data not shown). Thus, neither compromised apoptosis nor overt aneuploidy accounts for the accelerated lymphoma onset in Suv39h1-deficient Eμ-*myc* mice.

To directly assess oncogene-induced senescence as a potential component of delayed lymphoma manifestation, senescence-associated β-galactosidase (SA-β-gal) activity (Dimri et al., 1995) was analyzed in Suv39h1-deficient and control lymphomas. Virtually none of the cells in the *Suv39h1*$^{-}$ lymphoma sections, but an average of about 14% of the control lymphoma cells, stained (often in a focal pattern) positive for SA-β-gal ($P < 0.001$; Figures 1B and 1C; see Figures S1A and S1B available online for further evidence that senescent cells are indeed B lymphoma cells). Moreover, coanalysis of the proliferation marker Ki67 or bromodeoxyuridine (BrdU) incorporation, indicating DNA synthesis, with SA-β-gal or H3K9me3 staining confirmed the growth-arrested nature of SA-β-gal- or H3K9me3-positive cells (Figure 1D). Immunoblot analyses of bulk lymph node lysates indicated no differences in the expression levels of Myc and the cell-cycle inhibitor p21^{CIP1} between control and *Suv39h1*$^{-}$ lymphomas, while significant amounts of hypophosphorylated/G1-phase Rb and of H3K9me3 were only found in control lymphomas, which also displayed slightly reduced levels of the CDK4/6 inhibitor p16^{INK4a} and the E2F target cyclin A (Figure 1E). Other histone modifications such as H3K4me3, acetylated H3K9, H3K27me3, or H4K20me3 appeared globally unaffected by Suv39h1 status (data not shown), underscoring the specific role of the Suv39h1-mediated H3K9me3 mark in the senescence process. Moreover, spleen samples derived from young, lymphoma-free Eμ-*myc* mice (termed "preneoplastic," albeit consisting of Myc-overexpressing normal B cells) as compared with spleen sections from nontransgenic mice exhibited signs of cellular senescence in a strictly Myc- and Suv39h1-dependent fashion, indicating that oncogene-related senescence may delay tumorigenesis already at a premalignant state (Figure S1C). Thus, aggressive Myc-driven lymphomas develop and manifest with a significant fraction of cells that lack any proliferative activity and display marks of cellular senescence.

All Myc-lymphomas developing in *Suv39h1*$^{+/-}$;*p53*$^{+/-}$ or *Suv39h1*$^{-}$;*p53*$^{+/-}$ backgrounds selected against the remaining *p53* wild-type allele (12/12 cases tested "p53-null"; Figure 1F), as known from lymphomas forming in Eμ-*myc*;*p53*$^{+/-}$ mice (Schmitt et al., 1999), and, thus, against p53-dependent apoptosis. *Suv39h1* RNA expression was mostly retained in *Suv39h1*$^{+/-}$;*p53*$^{+/-}$-derived lymphomas (7/9 cases tested; Figure 1F), indicating that p53 loss coablates an apoptosis-independent tumor-suppressive function otherwise governed by Suv39h1. Accordingly, additional inactivation of *Suv39h1* produced no further acceleration of Eμ-*myc* lymphomagenesis in a *p53*$^{+/-}$ background (data not shown). Notably, and different from p53-null lymphomas, DDR-defective *ATM*$^{-/-}$ lymphomas displayed only a partial reduction of the senescent fraction at manifestation (Figure 1G and Figure S1D, showing, in addition, control lymphoma-comparable senescence in p16^{INK4a}-deficient *INK4a*$^{-/-}$ and p21^{CIP1}-deficient *CIP1*$^{-/-}$ lymphomas, but compromised senescence in *ARF*$^{-/-}$ lymphomas). Taken together, Myc-induced senescence presents in vivo as a p53-, Suv39h1-, and partly ATM-dependent program that complements apoptosis as an anti-oncogenic safeguard mechanism in Eμ-*myc* lymphomagenesis.

Activated Myc Promotes ATM/p53-Dependent Senescence

Myc activation is known to produce marks of DNA damage in vivo (Reimann et al., 2007), at least in part via ROS, which

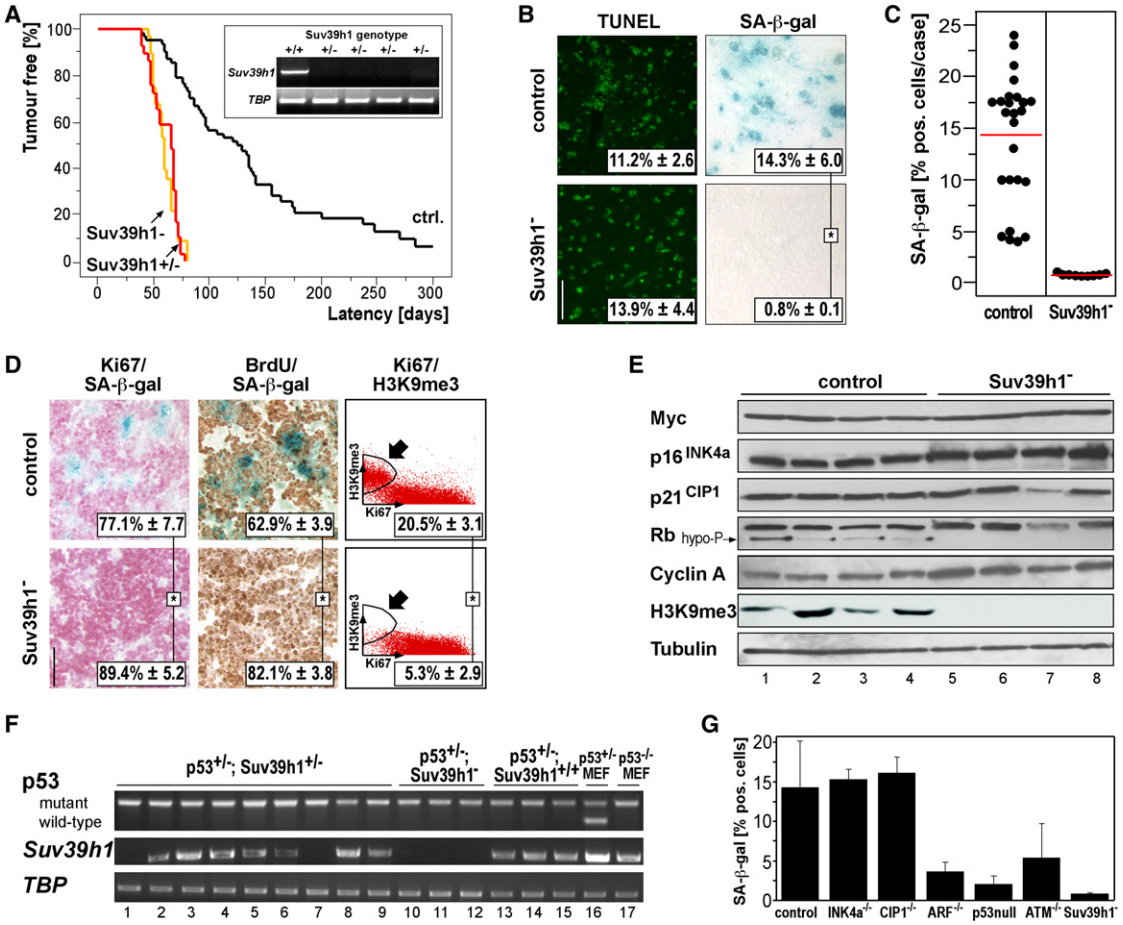

Figure 1. Suv39h1-Dependent Senescence Attenuates Myc-Driven Lymphomagenesis

(A) Latencies to palpable lymphoma manifestation in Eμ-*myc* transgenic mice (control lymphoma, n = 93, black), in Eμ-*myc*;*Suv39h1*$^{+/-}$ (n = 41, red), and in Eμ-*myc*;*Suv39h1*$^{-}$ mice (n = 31, orange). Insert: *Suv39h1* mRNA expression by RT-PCR analysis of short-term cultured lymphomas derived from *Suv39h1*$^{+/-}$ mice (n = 4) with a *Suv39h1*$^{+/+}$ derived lymphoma for comparison; *TBP* as an internal control.

(B) Growth-related parameters, i.e., apoptosis by TUNEL reactivity, and senescence by SA-β-gal staining in lymph node sections obtained at manifestation from Eμ-*myc* control or *Suv39h1*$^{-}$ lymphomas (representative photomicrographs from at least nine samples per genotype tested).

(C) Percentages of SA-β-gal-positive cells (as in B) in individual control (n = 25) and *Suv39h1*$^{-}$ (n = 9) lymphomas. Horizontal lines represent the mean percentage of each group. Note that low-level SA-β-gal-positive cases in the control group are enriched for spontaneously *p53* mutant or homozygously *INK4a/ARF*-deleted lymphomas (Schmitt et al., 1999) (data not shown).

(D) Percentages of Ki67-positive (red) and BrdU-positive cells (brown; note the mutually exclusive SA-β-gal-costaining [blue]) in situ, and quantification of H3K9me3^{high}/Ki67^{low} cells (arrow-marked gate, representing senescent cells) by flow cytometry in control and *Suv39h1*$^{-}$ lymphomas.

(E) Immunoblot analyses of the indicated proteins in individual control (lanes 1–4) and *Suv39h1*$^{-}$ (lanes 5–8) lymphoma cell lysates with α-tubulin as a loading control (arrow indicates the hypophosphorylated [hypo-P] Rb band representing cells in G1).

(F) Genomic status of the *p53* locus by allele-specific PCR (top) and expression status of *Suv39h1* transcripts by RT-PCR (bottom; *TBP* as an internal control) analyses of short-term cultured lymphoma cells that were isolated from mice of the indicated genotypes. Extracts from *p53*$^{+/-}$ and *p53*$^{-/-}$ MEFs as controls.

(G) Frequencies of SA-β-gal-positive cells in Eμ-*myc* lymphoma cryosections of the indicated genotypes at diagnosis (control and *Suv39h1*$^{-}$ as in B, at least four cases per genotype tested). All numbers indicate the mean percentages of positive cells ± SD; *p < 0.05. All scale bars represent 50 μm (identical magnification throughout the panel). See also Figure S1.

may link Myc via a DDR to Suv39h1-dependent senescence. Notably, Suv39h1 had no impact on γ-H2AX-marked DNA lesions and the DDR signature in preneoplastic Eμ-*myc* transgenic B cells, or in lymphoma cells exposed to γ-irradiation (Figure S2A-C). However, in contrast to wild-type B cells, primary B cells lacking the DDR mediators ATM or p53 largely failed—like Suv39h1-deficient B cells—to senesce in response to acute Myc overexpression in vitro (Figure 2A. If senescence detected in control lymphomas in situ is initiated via a Myc-evoked DDR, then genetic or pharmacological interference with the DDR should impact on the senescence response. Comparable to the *ATM*$^{-/-}$ scenario (Figure 1G), exposure of Eμ-*myc* transgenic mice to the ROS scavenger N-acetyl-cysteine (NAC) or to the ATM/ATR inhibitor caffeine, both of which blunt an oncogene-evoked DDR in vivo (Bartkova et al., 2006; Reimann et al., 2007), resulted in a profound, albeit only partial reduction of senescent lymphoma cells in situ (Figure S2D-F, also showing that ROS levels are Myc, but not Suv39h1 dependent).

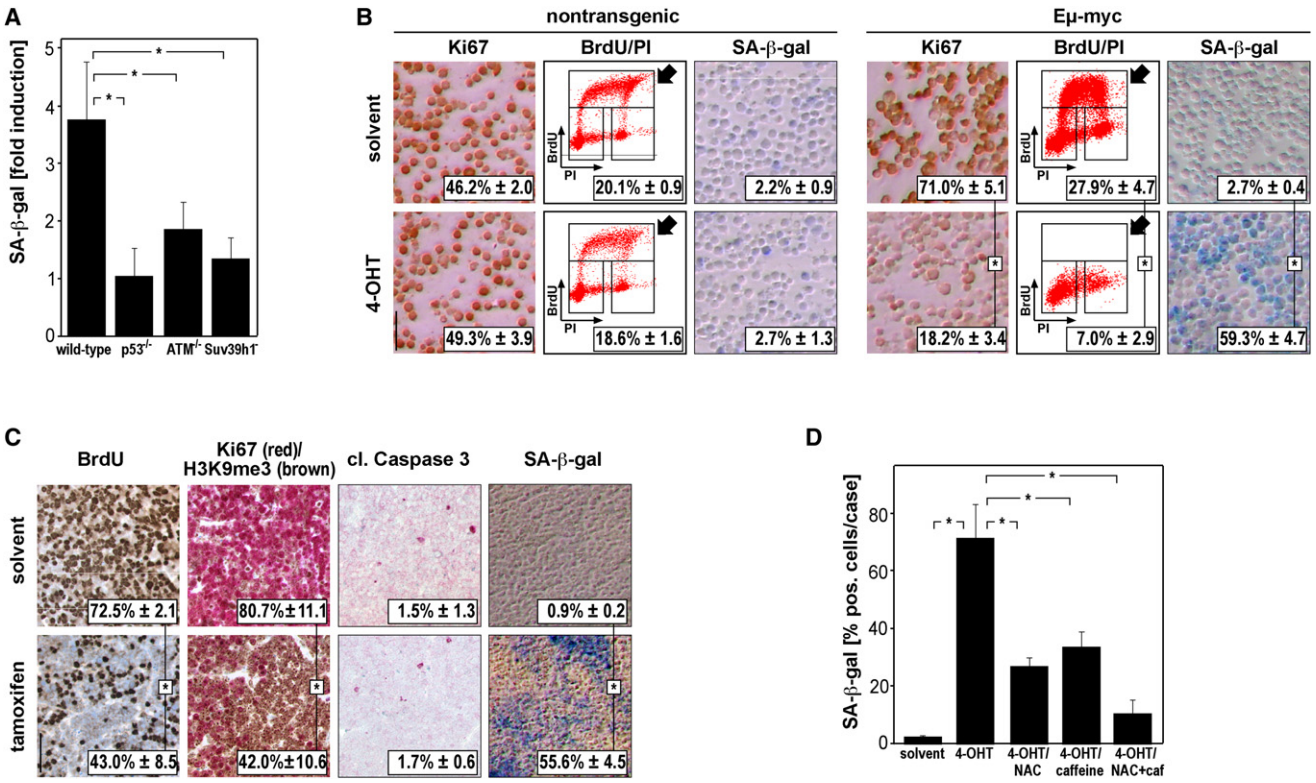

Figure 2. Myc Has p53-Dependent Prosenescent Potential

(A) Relative fractions of SA-β-gal-positive nontransgenic primary B cells of the indicated genotypes 10 days after stable transduction with a Myc construct (≥ 80% of the cells infected; dead cells [around 40% initial apoptosis] were removed, resulting in about 5% senescent cells in the wild-type population) as compared with an empty vector.

(B) Growth parameters (i.e., Ki67, S-phase fraction by BrdU/PI [arrow], and SA-β-gal frequencies) in *bcl2*-infected nontransgenic B cells (left) and Eμ-*myc*; *p53ER*$^{TAM/(-)}$/*bcl2* lymphoma lymphomas (right) in which functional p53 is restored in response to 4-OH-tamoxifen (4-OHT; solvent serving as the negative control) treatment for 6 days. Scale bar represents 20 μm (identical magnification throughout the panel).

(C) Acute induction of functional p53 by administration of tamoxifen in mice bearing lymphomas as in (B); stained for BrdU labeling, Ki67 reactivity (H3K9me3: 10.7% ± 3.5 [solvent] versus 39.0% ± 6.2 [tamoxifen]), apoptosis-indicating cleavage (cl.) of caspase 3, and SA-β-gal activity. Scale bar represents 50 μm (identical magnification throughout the panel).

(D) SA-β-gal frequencies in lymphomas as in (B) exposed in vitro for 6 days to 4-OHT (or a solvent as negative control) with no additional compound, or 5 mM of the ATM/ATR inhibitor caffeine (caf), 5 mM of the ROS scavenger N-acetyl-cysteine (NAC), or both. At least three cases each in all these experiments; all numbers indicate the mean percentages of positive cells ± SD; *p < 0.05. See also Figure S2.

To directly address the cell-autonomous potential of Myc to drive senescence, we tested whether a conditional p53 moiety would suffice to convert constitutive Myc signaling into a robust senescence response in apoptosis-incapable cells. To this end, we employed Eμ-*myc* mice carrying a 4-OH-tamoxifen (4-OHT)-inducible *p53ER*^{TAM} knockin allele, encoding a p53-estrogen receptor fusion protein that is inactive in the absence of 4-OHT (Martins et al., 2006). Expectedly, Eμ-*myc*;*p53ER*$^{TAM/+}$ lymphomas that arose in the absence of 4-OHT typically selected against the remaining *p53* wild-type allele (termed *p53ER*$^{TAM/(-)}$; 5/5 cases tested (data not shown and Martins et al., 2006), thereby generating p53-null lymphomas in which p53 activity is restorable upon provision of 4-OHT (Figure S2G). Constitutively Myc-expressing and *bcl2*-transduced (and, thus, apoptosis-protected) lymphoma cells quantitatively entered senescence following exposure to 4-OHT in vitro, whereas nontransgenic Bcl2-protected p53ER^{TAM}-expressing B cells lacked such a response (Figure 2B). Similarly, senescence was strongly induced when mice harboring Eμ-*myc*;*p53ER*$^{TAM/(-)}$/*bcl2* lymphomas were exposed to tamoxifen in vivo (Figure 2C). Importantly, pharmacological scavenging of ROS or ablation of the DDR attenuated and, when combined, almost completely blocked the senescence induction of Eμ-*myc*;*p53ER*$^{TAM/(-)}$/*bcl2* lymphoma cells in response to 4-OHT in vitro (Figure 2D). Thus, acute overexpression of Myc in primary cells or p53 reactivation in the presence of constitutive Myc signaling unmasks the cell-autonomous, DDR-mediated prosenescent capability of Myc.

TGF-β Induces Senescence of Myc-Driven Lymphoma Cells

Because neither ATM deficiency nor pharmacological DDR ablation was sufficient to fully abrogate senescence of Myc-driven lymphoma cells in vivo, we aimed to identify an additional stimulus that may complement oncogene-induced DDR signaling in vivo. Genome-wide transcriptional profiling of whole lymph node RNA preparations from Suv39h1-proficient versus Suv39h1-deficient Eμ-*myc* lymphomas identified *TGF-β-induced gene* (*Tgfbi*; also known as Big-h3, β-ig H3, or keratoepithelin) as

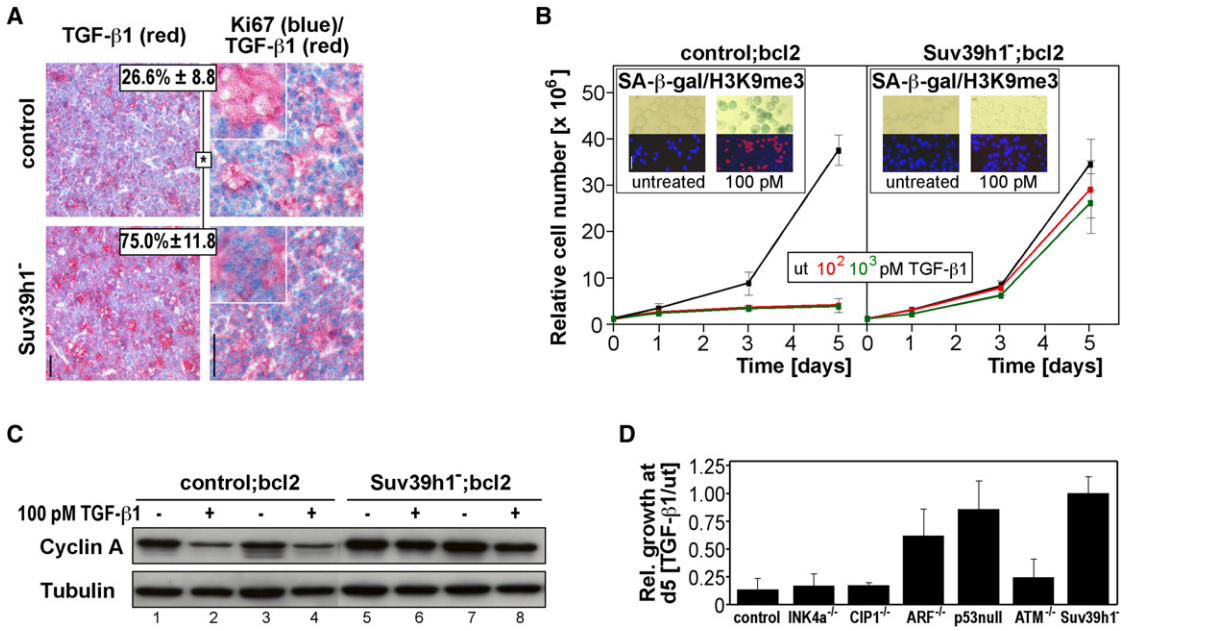

Figure 3. TGF-β Induces Suv39h1-Dependent Cellular Senescence in Myc-Driven Lymphomas

(A) Focal TGF-β1 detected by immunostaining (left) and costaining (right) for TGF-β1 (red) and Ki67 (blue) in control versus *Suv39h1*$^-$ lymphomas in lymph node sections in situ (representative photomicrographs). Inserts show TGF-β1-rich areas at higher magnification, and percentages reflect the fraction Ki67-positive cells within those areas (n = 3 samples each). Scale bar represents 50 μm (identical magnification throughout the panel).

(B) Growth curve analyses of freshly isolated and stably *bcl2*-infected control and *Suv39h1*$^-$ lymphoma cells exposed to the indicated concentrations of TGF-β1 (100 pM [red], 1000 pM [green]) or left untreated (black); n = 5 each. Inserts show untreated versus TGF-β1-exposed (100 pM; day 5) lymphoma cell cytospin preparations assayed for SA-β-gal (top; 50.0% ± 13.2 [control] versus 3.3% ± 2.9 [*Suv39h1*$^-$] for TGF-β1) and H3K9me3 reactivity (bottom; in red with DAPI as counterstain; 35.4% ± 14.4 [control] versus 0.4% ± 0.1 [*Suv39h1*$^-$] for TGF-β1). Note the comparable proliferative capacities of Suv39h1-proficient and Suv39h1-deficient lymphoma cells in the absence of TGF-β1 treatment. Scale bar represents 10 μm (identical magnification throughout the panel).

(C) Immunoblot analysis of cyclin A protein levels (α-tubulin as a loading control) in lymphomas as in (B) with or without preceding exposure to TGF-β1 (100 pM for 5 days).

(D) Relative growth of Bcl2-expressing lymphoma cells of the indicated genotypes after 5 days of exposure to TGF-β1 (100 pM) versus untreated (as in [B]). At least three cases each. Error bars denote SD; *$p < 0.05$. See also Figure S3.

the most strongly differentially upregulated transcript. *Tgfbi*, a TGF-β target, was expressed 3.9-fold higher in *Suv39h1*$^-$ lymphomas, and encodes a secreted protein with cytostatic potential that was previously linked to cellular senescence (Dokmanovic et al., 2002) (see Experimental Procedures for details and the confirmatory quantitative reverse transcriptase polymerase chain reaction [RQ-PCR] analysis in Figure S3A). We found TGF-β1, known to induce cellular senescence in fibroblasts (Lin et al., 2004), to be detectable in a multi-focal pattern in lymphoma sections reminiscent of the distribution of SA-β-gal-positive cells in control lymphomas (Figure 3A, compare to Figure 1B). Importantly, costaining for the proliferation marker Ki67 unveiled that in areas with abundant TGF-β1 significantly less control cells were Ki67-positive when compared with *Suv39h1*$^-$ lymphomas (Figure 3A). Thus, TGF-β correlates with a cytostatic response selectively detectable in control lymphomas, and high *Tgfbi* levels in *Suv39h1*$^-$ cells are suggestive of a downstream defect in a TGF-β-inducible senescence program.

We sought to directly test the potential of exogenous TGF-β1 to induce cellular senescence in a Suv39h1-dependent fashion in Myc-driven lymphoma cells that were stably *bcl2*-transduced to block apoptosis. TGF-β1 countered proliferation in a dose-dependent manner and led to a complete growth arrest with features of cellular senescence, i.e., SA-β-gal activity and H3K9me3 expression, in control, but not in *Suv39h1*$^-$ lymphoma cells, whose growth behavior remained largely unaffected by TGF-β1 treatment (Figure 3B). Lack of a cytostatic response in *Suv39h1*$^-$ cells was not due to a primary defect in TGF-β receptor signaling, because lymphoma cells of both genotypes exhibited phosphorylation of the intracellular TGF-β1 mediators Smad2 and Smad3 following TGF-β1 treatment in vitro (Figure S3B). In line with the transcriptionally repressive H3K9me3 mark selectively induced in control lymphomas (Figure 3B), TGF-β1-treated control lymphomas displayed reduced transcript levels of numerous E2F target genes, including *MCM7* or *Cyclin A* by microarray analysis, as well as increased levels of transcripts that encode for components of the heterochromatinization machinery such as *DNA methyltransferase 3B* or *HP1β* (Figure S3C, and Figure 3C for cyclin A protein expression). The mechanism by which TGF-β utilizes Suv39h1, presumably in conjunction with Rb/E2F complexes (Laiho et al., 1990; Schwarz et al., 1995; Spender and Inman, 2009), to induce senescence appears to be indirect, because we were unable to detect a physical interaction between Suv39h1 and Smad proteins (Figure S3D). TGF-β1 was incapable of inducing $p15^{INK4b}$ or $p21^{CIP1}$ mRNA and protein expression in lymphomas independent of their Suv39h1 status, probably because constitutive Myc expression firmly represses these promoters via Miz-1

(Seoane et al., 2002; Spender and Inman, 2009) (Figure S3E, and transcriptional levels by RQ-PCR, data not shown). Unlike γ-irradiation, TGF-β1 treatment of lymphoid cells failed to produce DNA lesions (Figures S3F and S3G), and was not accompanied by elevated ROS levels either (data not shown). Of note, H_2O_2-induced DNA damage, at levels comparable to DNA damage evoked by oncogenic Myc, synergized with TGF-β to promote cellular senescence (Figure S3G, compare with γ-H2AX foci in Figure S2A), as seen for Myc induction and TGF-β treatment in MEFs (Figure S3H). Accordingly, DDR-defective *ATM*$^{-/-}$ lymphomas senesced in response to TGF-β1 as control (or, likewise, $p16^{INK4a}$- or $p21^{CIP1}$-deficient) lymphomas did, whereas p53-null lymphomas were expectedly refractory (Cordenonsi et al., 2003) (Figure 3D). Hence, TGF-β promotes cellular senescence without damaging DNA, but cooperatively with oncogene-related DDR signaling in a Myc-primed and p53/Suv39h1-dependent fashion.

Next, we aimed to identify the cellular source of the considerable amounts of TGF-β detectable in Eμ-*myc* lymphoma tissues. Importantly, lymphoma cells did not secrete TGF-β1 above culture medium background levels (Figure S3I). However, freshly isolated lymphoma cells exhibited Smad3 phosphorylation (Smad3-P), a mark of activated TGF-β signaling, whereas Smad3-P was undetectable in freshly isolated preneoplastic Eμ-*myc* transgenic B cells (Figure S3J; see also Figure S1C). Likewise, no Smad3-P signal was found in nontransgenic B cells following transduction with a Myc expression construct, indicating that Myc per se is incapable of driving TGF-β expression. Notably, the recently observed link between oncogene-induced senescence and a senescence-reinforcing proinflammatory secretory phenotype, termed "SASP" (Acosta et al., 2008; Coppe et al., 2008; Kuilman et al., 2008; Wajapeyee et al., 2008), raised the question of whether TGF-β1 might be a component or a regulator of the SASP-related cytokines. However, RQ-PCR analysis of a panel of SASP candidates in Myc-lymphomas of various genotypes exposed to senescence-inducing H_2O_2 or TGF-β1 unveiled substantial SASP induction only in senescence-capable control lymphomas following exposure to H_2O_2, but not to TGF-β1. Moreover, TGF-β1 itself does not belong to the SASP signature of lymphoma cells, which is different from fibroblasts that expressed increased amounts of TGF-β1 upon γ-irradiation or H_2O_2 (Figure S3K-M). In essence, neither proliferating nor senescent lymphoma cells secrete significant amounts of TGF-β, implying that TGF-β might be provided by nonneoplastic bystander cells.

Apoptotic Lymphoma Cells Activate Macrophages to Secrete Prosenescent TGF-β1

We considered lymphoma-infiltrating and lymphoma-activated macrophages to serve as a non-cell-autonomous source of TGF-β1 in vivo, because macrophages reportedly secrete TGF-β1 upon phosphatidylserine (PS)-dependent ingestion of apoptotic cells (Huynh et al., 2002; Savill and Fadok, 2000), which are typically found at significant frequencies in Myc-driven lymphomas (Figure 1B, and Figure S4A for the phenotypic characterization of lymphoma-infiltrating macrophages). Indeed, coculture of macrophages with PS-positive apoptotic, but not with PS-negative proliferating, lymphoma cells resulted in increased TGF-β1 secretion, as alternatively observed upon stimulation of macrophages with PMA (phorbol 12-myristate 13-acetate; Figure 4A and Figure S4B). Consistently, lymphomas harboring a robust Bcl2-mediated apoptotic block (control/bcl2; see also Schmitt et al., 2002b) presented with a much lower frequency of both infiltrating macrophages and senescent cells in vivo (Figure 4B and Figure S4C, see also Figure 1G and Figure S1D for a correlation between senescent cells and infiltrating macrophages in various lymphoma genotypes). The nearly complete absence of senescent control;bcl2 lymphoma cells in vivo despite their in vitro susceptibility to TGF-β-mediated senescence (Figure 3B) underscores the importance of non-cell-autonomous events such as attraction of macrophages (Lauber et al., 2003) and their subsequent activation by apoptotic lymphoma cells to secrete TGF-β1.

To further elucidate the prosenescent role of activated macrophages in vivo, we adoptively transferred PMA-stimulated Ana-1 macrophages into mice harboring Myc-driven lymphomas. GFP-tagged Ana-1 cells homed to lymphoma sites, and their presence correlated with enhanced TGF-β1 pathway activation (i.e., Smad3-P), induction of the TGF-β target and senescence indicator plasminogen activator inhibitor-1 (PAI-1), and, most notably, with a substantial increment of senescent lymphoma cells (Figure 4C, and Figures S4D and S4E). Conversely, systemic depletion of macrophages by repetitive provision of liposome-encapsulated clodronate (Aichele et al., 2003) significantly lowered the number of lymphoma-infiltrating macrophages, Smad3 activation (i.e., Smad3-P), and, most importantly, lymphoma cell senescence (Figure 4D, and Figures S4F and S4G; for effects of pharmacological inhibition of TGF-β production see Figures S4H–S4J).

To confirm the impact of TGF-β on senescence induction in vivo, we sought to locally block its action by expressing a soluble, secretable TGF-β1-neutralizing TGF-β type II receptor extracellular domain (TβR-II-ED), thereby restricting TGF-β inhibition to the vicinity of TβR-II-ED-expressing cells (Thomas and Massague, 2005). Importantly, transplantation of Eμ-*myc* transgenic hematopoietic stem cells stably transduced with TβR-II-ED into lethally irradiated recipient mice resulted in a profoundly accelerated onset of lymphomas ($p < 0.0001$); these lymphomas virtually lacked Smad3 phosphorylation and displayed, despite unaffected macrophage frequencies, much fewer senescent cells when compared with a mock-infected cohort (Figure 4E and 4F and Figures S4K–S4M). Tumor latency remained unchanged when the TβR-II-ED moiety was tested in Suv39h1-deficient hematopoietic stem cells, indicating that TGF-β-mediated apoptosis has no significant tumor-delaying impact in this model (data not shown). Furthermore, when matched pairs of primary lymphomas were propagated in immunocompetent recipients, TβR-II-ED-expressing lymphomas always formed with lower senescence frequencies than the corresponding empty vector samples (Figure 4G). Thus, selective ablation of TGF-β action reduces lymphoma cell senescence in tumor development and in otherwise genetically identical lymphoma aliquots during tumor expansion in vivo. Importantly, these results, like the sharply reduced senescence frequency in Bcl2-protected lymphomas in vivo (Figure 4B), clarify that the non-cell-autonomous induction of senescence is quantitatively substantially more relevant than the cell-autonomous signaling cascade into senescence (as addressed in Figure 2).

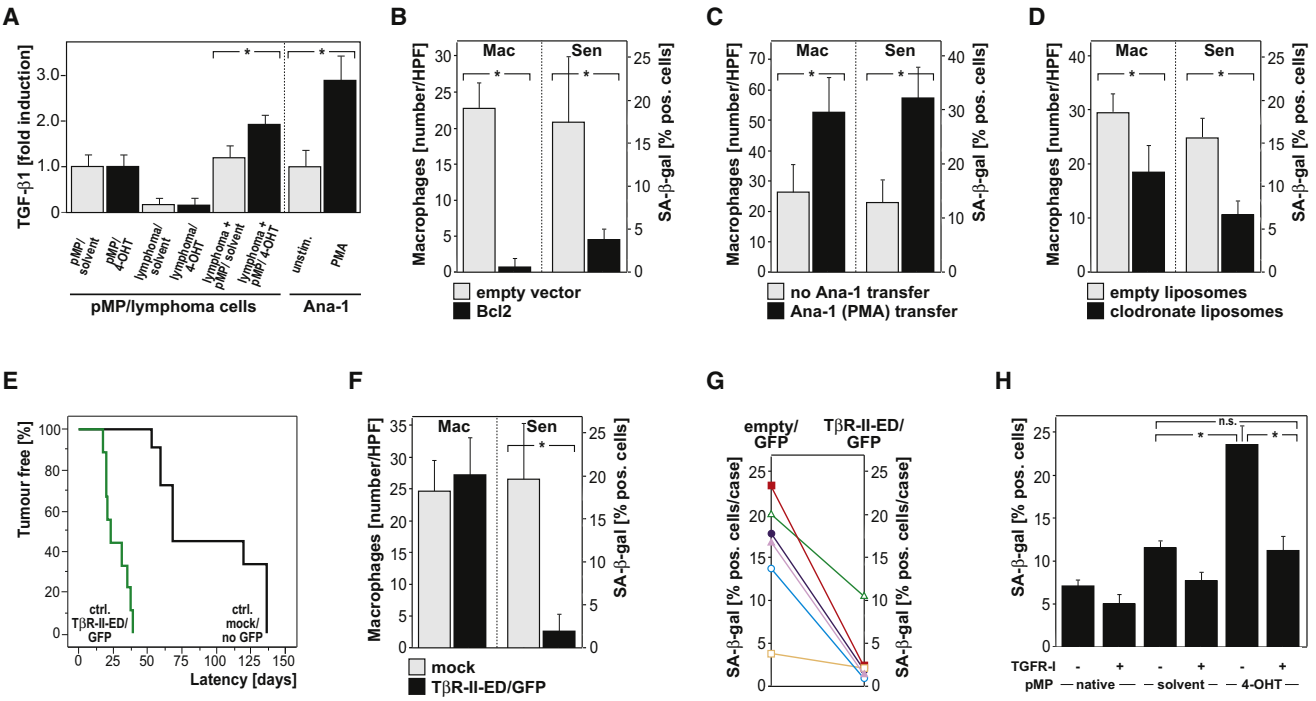

Figure 4. Environmental TGF-β, as Secreted by Apoptotic Lymphoma Cell-Activated Macrophages, Accounts for Lymphoma Cell Senescence In Vivo

(A) Relative induction of TGF-β1 protein levels at 48 hours by enzyme-linked immunosorbent assay in cell culture supernatants of primary peritoneal macrophages (pMP) alone or after coculture with Eμ-*myc*;*p53ER*$^{TAM/(-)}$ lymphomas exposed for 20 hours to 4-OHT or solvent (n = 3 each; relative to the normalized medium-corrected "pMP solvent" value). Note that 4-OHT, but not solvent, quantitatively produced PS-positive apoptotic lymphoma cells (Figure S4B). Relative induction of TGF-β1 secretion at 48 hours by PMA-stimulated (200 ng/ml) Ana-1 macrophages for comparison (in triplicate).

(B–D) Quantification of macrophage infiltration (Mac) measured by F4/80 immunostaining (numbers indicating average macrophage count per high-power field) and of senescence (Sen) assessed by SA-β-gal staining (B) in apoptosis-blocked Bcl2-expressing lymphomas, generated by retroviral *bcl2* transfer (or an empty vector as control) into Eμ-*myc* transgenic fetal liver cells and their subsequent propagation in lethally irradiated recipients, at manifestation, (C) following adoptive transfer of PMA-stimulated Ana-1 macrophages (as in A) by intravenous transfer into control lymphoma bearing mice, and (D) after systemic monocyte/macrophage depletion by liposome-encapsulated clodronate or empty liposomes for comparison.

(E) Tumor latencies, stratified by lymphoma GFP expression, in lethally irradiated recipients of Eμ-*myc* transgenic fetal liver cells stably transduced with the MSCV-TGF-β receptor type II ecto domain-IRES-GFP (TβR-II-ED/GFP) retrovirus (TβR-II-ED/GFP-positive, n = 9, green, versus mock/GFP-negative, n = 11, black).

(F) Quantification of macrophage infiltration and senescence, assessed as in (B-D), in TβR-II-ED/GFP-expressing versus mock-infected lymphomas as in (E). Note that around 10%–20% of the overall senescence frequency can be attributed to the cell-autonomous component (see also B).

(G) Matched pair quantification of cellular senescence in individual control lymphomas (n = 6) infected with the TβR-II-ED/GFP or an empty/GFP retrovirus that formed after sorting and transplantation of GFP-expressing cells.

(H) Senescence frequencies of *bcl2*-infected control lymphoma cells exposed—in the presence or absence of the TGF-β receptor type I inhibitor SD-208 (TGFR-I; 500 nM) —to pMP that were either native or cocultivated with Eμ-*myc*;*p53ER*$^{TAM/(-)}$ lymphomas plus solvent or 4-OHT for 48 hours. All experiments in this figure represent at least three independent samples each; all numbers indicate mean values ± SD; *p < 0.05; n.s., indicates not significant. See also Figure S4.

Ultimately, we aimed to dissect the sequential process of lymphoma cell apoptosis-induced macrophage-derived TGF-β action on lymphoma cell senescence in a single in vitro experiment. To this end, we coincubated Bcl2-protected lymphoma cells with macrophages, which were activated by exposure to apoptotic lymphoma cells beforehand, with or without a pharmacological TGF-β receptor type I inhibitor (TGFR-I). Indeed, only apoptotic body-activated macrophages produced a more than 3-fold increase of SA-β-gal-positive lymphoma cells that was largely abolished in the presence of the TGFR-I (Figure 4H and Figure S4N). Therefore, TGF-β secreted by macrophages upon their activation by apoptotic lymphoma cells indeed acts as a critical stroma-derived inducer of lymphoma cell senescence.

To test whether the proposed mouse model-deduced mechanism of non-cell-autonomous senescence induction may apply to human aggressive B cell lymphomas as well, we analyzed its central components in a panel of 30 diffuse large B cell lymphoma samples. The panel was subdivided based on Ki67 immunoreactivity into a very high proliferation (Ki67^{hi}; ≥ 80% Ki67-positive cells) group and a lower proliferation (Ki67^{lo}; < 80% Ki67-positive cells) group. Indeed, Ki67^{lo} samples exhibited a significantly higher frequency of H3K9me3-positive cells, indicative of cellular senescence in paraffin-embedded sections that cannot be examined for enzymatic SA-β-gal activity (Figure 5A and 5B). Importantly, the Ki67^{lo} group also presented with a higher fraction of apoptotic cells, more lymphoma-infiltrating macrophages, and a stronger reactivity for the TGF-β signaling mediator

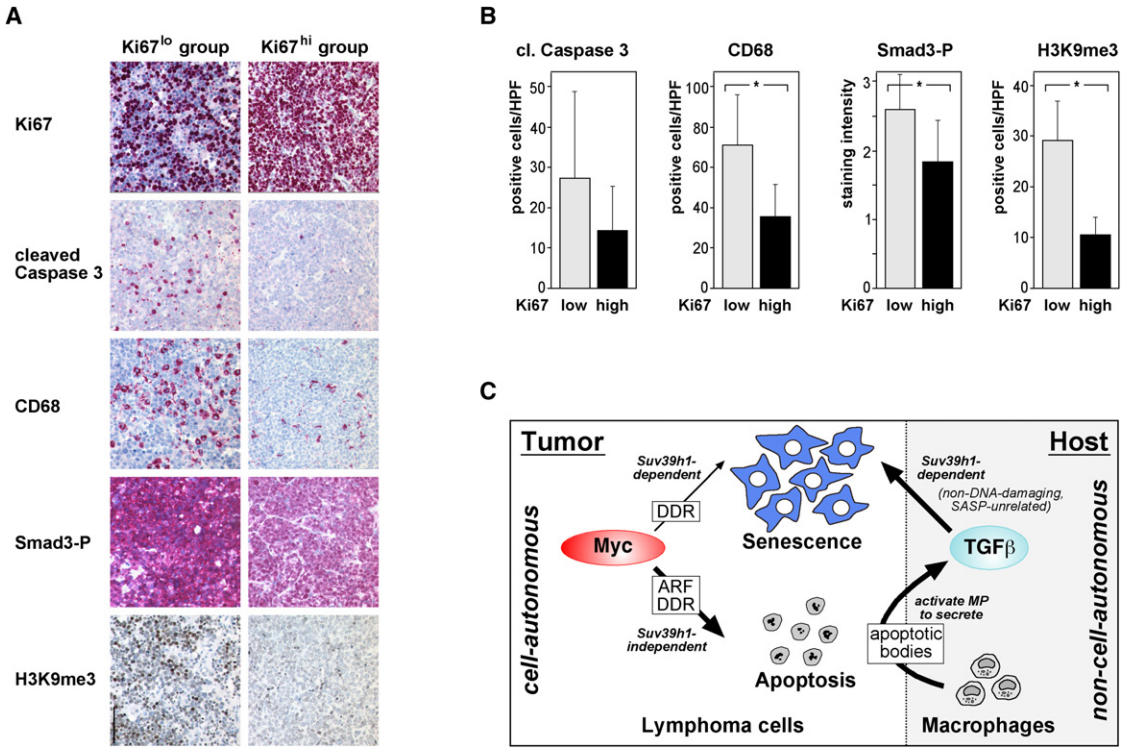

Figure 5. Human Diffuse Large B Cell Lymphomas (DLBCL) Display Features Consistent with the Model of Non-Cell-Autonomous TGF-β-Mediated Cellular Senescence

(A) Two DLBCL cases reflecting a highly (Ki67^{hi}; samples with ≥ 80% Ki67-positive cells) and a less intensely proliferating (Ki67^{lo}; samples with < 80% Ki67-positive cells) subgroup also stained for apoptosis (cleaved Caspase 3), macrophage infiltration (CD68), TGF-β pathway activation (i.e., Smad3-P), and cellular senescence (i.e., H3K9me3 as a surrogate marker). Representative photomicrographs of a total of 30 cases analyzed. Scale bar represents 100 μm (identical magnification throughout the panel).

(B) Quantitative assessment of cleaved (cl.) Caspase 3, CD68, Smad3-P, and H3K9me3 in the Ki67 low versus high groups (Ki67^{lo}, n = 19, Ki67 reactivity 68.7% ± 6.6 versus Ki67^{hi}, n = 11, 88.9% ± 5.7; $p < 0.001$). All comparisons are highly statistically significant (i.e., $p < 0.001$), except a trend ($p = 0.07$) for cl. caspase 3. All numbers indicate mean values ± SD; *$p < 0.05$. Notably, no clear association of the Ki67 status with the germinal center (GC) B cell-of-origin status (GCB versus non-GCB by immunostaining [Hans et al., 2004], data not shown) was observed.

(C) Model of oncogene-initiated cell-autonomous and non-cell-autonomous cellular senescence in aggressive B cell lymphomas, as concluded from Eμ-*myc* mouse lymphoma data.

Smad3-P (Figure 5B). Thus, these data strongly suggest that environmentally cocontrolled tumor cell senescence plays an important growth-restraining role in human aggressive B cell lymphomas as well.

DISCUSSION

Our data establish a model of senescence induction in an oncogenic context where the primary cellular response to the driving oncogene is overt apoptosis, not senescence. Elegant work elucidating signaling cascades involved in RAS-, BRAF-, or MEK-type oncogene-induced senescence demonstrated that an oncogene-evoked DDR (Bartkova et al., 2006; Di Micco et al., 2006; Mallette et al., 2007), a global negative feedback response attenuating RAS effector signaling (Courtois-Cox et al., 2006), and, most recently, proinflammatory cytokines acting as reinforcing networks (Acosta et al., 2008; Coppe et al., 2008; Kuilman et al., 2008; Wajapeyee et al., 2008) contribute to the senescence phenotype. However, all of these studies view senescence as a cell-autonomous phenomenon in which, if at all, cellular interactions or secreted factors promote the senescent arrest in a homotypic self-amplifying way. We report here an oncogene-initiated but non-cell-autonomous route into senescence. This process depends on the activation of TGF-β1-secreting nonneoplastic cells as a critical intermediate step, linking Myc-provoked cell-autonomous apoptosis to the subsequent senescence induction of a significant proportion of the remaining tumor cells by the stromal cytokine (Figure 5C). Hence, our data demonstrate that apoptosis and senescence are not simply two context-dependent choices of cellular stress responsiveness, but that they can be enforced in an interdependent fashion on the organismic level. In this regard, disrupted DNA damage signaling might not only compromise cell-autonomous induction of cellular senescence (Figures 1G and 2D and Figures S2E and S2F), but might also anticipate impaired macrophage-related senescence due to reduced primary apoptosis. Importantly, DDR-defective tumor cells remain susceptible to non-DNA-damaging prosenescent stimuli that might be therapeutically exploited in the future. Moreover, our data underscore why p53 inactivation—blocking apoptosis,

preventing macrophage attraction, and rendering the cell insensitive to TGF-β-induced senescence—is a particularly efficient way to escape Myc-related senescence.

We would like to emphasize that 12%–20% senescent cells, which were detectable in control lymphomas at diagnosis, are indeed likely to account for a substantial delay in tumor formation. These frequencies reflect "snapshots" of a dynamic process that involves rapid clearance of senescent cells by the host immune system (J.R.D. and C.A.S., unpublished data), as recently reported for a mouse model presenting with senescent liver cancer cells (Xue et al., 2007). The profound impact on overall tumor growth of relatively small steady-state proportions of cells that exited the cycle is well established in the apoptosis field and seems to apply to senescent cells in a comparable way.

Of note, cellular and secreted components that delay tumor manifestation via senescence as shown here do not necessarily keep operating as tumor constraints during later steps of cancer progression, because there is ample evidence that both tumor-associated macrophages and TGF-β can produce deleterious effects by promoting tumor growth or by exerting tolerogenic immune effects (Dave et al., 2004; Thomas and Massague, 2005). However, TGF-β1 signaling has just been reported as a component of the prognostically favorable "stromal-1" signature in human diffuse large B cell lymphoma (Lenz et al., 2008), a frequently Myc-activated entity in which we identified here a subgroup with features highly reminiscent of the presented mechanism of macrophage-mediated senescence induction that we genetically dissected in the murine Eμ-*myc* model of aggressive B cell lymphoma.

Furthermore, our findings characterize the Rb-related Suv39h1-mediated H3K9me3/HP1 heterochromatin mark as a rather universal and essential downstream effector module of the senescence program that is still operational in the presence of constitutive Myc signaling. This chromatin mark is produced not only by activated oncogenes or DNA damaging chemotherapy (Braig et al., 2005; Collado et al., 2005; Michaloglou et al., 2005), but also by the cytostatic action of secretory TGF-β. Given the anticancer relevance of cellular senescence, the now demonstrated inducibility of senescence by a non-DNA-damaging cytokine opens the exciting perspective to utilize Suv39h1/H3K9me3-enforcing approaches for future cancer therapies.

EXPERIMENTAL PROCEDURES

Lymphoma Analysis and In Vivo Treatments

The use of human tumor biopsies primarily obtained for the initial diagnosis of diffuse large B cell lymphoma as anonymous samples was based on informed patient consent, and was specifically approved by the local ethics commission of Charité - Universitätsmedizin Berlin (reference EA4/085/07).

All animal protocols used in this study were approved by the governmental review board (Landesamt Berlin), and conform to the respective regulatory standards. Lymphomas with defined genetic defects were generated by intercrossing Eμ-*myc* transgenic mice with mice carrying loss-of-function alleles at the *Suv39h1*, the *p53*, the *INK4a/ARF*, the *CIP1*, or the *ATM* locus, all in a C57BL/6 background (Adams et al., 1985; Barlow et al., 1996; Christophorou et al., 2005; Deng et al., 1995; Jacks et al., 1994; Kamijo et al., 1997; Krimpenfort et al., 2001; Peters et al., 2001). Genotyping of the offspring by allele-specific genomic PCR, monitoring of lymphoma onset, preservation of snap-frozen or formalin-fixed lymph node tissue and isolation of viable lymphoma cells, splenic B-lymphocytes (via magnetic bead selection [B cell isolation kit, Miltenyi]), fetal liver cells (FLC), primary peritoneal macrophages (pMP), or mouse embryo fibroblasts (MEF) were carried out as described (Davies and Gordon, 2005; Reimann et al., 2007; Schmitt et al., 2002a, 2002b). Where indicated, B cells were prestimulated for 48 hours with 5 μg lipopolysaccharide (LPS)/ml (from Salmonella enterica; Sigma-Aldrich). Preneoplastic cells were obtained from approximately 30-day-old Eμ-*myc* transgenic animals devoid of lymph node or spleen enlargement and with no evidence of leukemia by blood smear analysis. In some experiments, mice were exposed to specific drug treatments as described in the Supplemental Experimental Procedures.

Eμ-*myc* transgenic FLC as a source of hematopoietic stem cells were obtained to reconstitute (sublethally, i.e., a single 6 or 10 Gy dose of total body γ-irradiation) irradiated nontransgenic recipient mice. FLC, splenic B-lymphocytes, isolated lymphoma cells (typically on irradiated NIH3T3 fibroblasts serving as feeders), macrophages, and MEFs were cultured in liquid medium or semisolid methylcellulose as described (Schmitt et al., 1999, 2000), and stably transduced with MSCV-c-Myc-IRES-GFP, MSCV-HA-Suv39h1-puro (kindly provided as pcDNA3.1-HA-Suv39h1 by A. Leutz), MSCV-bcl2-blasticidine, MSCV-bcl2-puro, pBabe-c-MycER^{TAM}-puro (a generous gift from M. Eilers), or the GFP coencoding retroviruses MSCV-IRES-GFP and MSCV-TβR-II-ED-IRES-GFP (kindly provided as MSCV-TβR-II-ED-puro by J. Massagué) (Reimann et al., 2007; Schmitt et al., 1999, 2002b); the C57BL/6-derived Ana-1 macrophages (kindly provided by L. Varesio) were GFP-transduced via nucleofection (nucleofector kit V, Lonza). In some settings, macrophages were treated in vitro with phorbol 12-myristate 13-acetate (PMA; Sigma), lisinopril, or adriamycin (Sigma) for the indicated times and at the indicated concentrations.

Analysis of Growth Parameters, Chromosomal Abnormalities, and DNA Damage

In some experiments, lymphoma cells were exposed in vitro to purified human TGF-β1 (R&D Systems) at 100 or 1000 pM, or were treated with 1 μM 4-hydroxy-tamoxifen (4-OHT; Sigma-Aldrich) or the equivalent volume of the ethanol-based solvent, or were incubated with H_2O_2 (100 μM; Sigma-Aldrich), or were exposed to the TGF-β R I inhibitor V (SD-208; 500 nM; Calbiochem/Merck) for the indicated times, or were treated with NAC or caffeine (Sigma-Aldrich) as stated. Viability and cell numbers were analyzed by trypan blue dye exclusion, cell-cycle parameters by BrdU and propidium iodide (PI) staining (Schmitt et al., 1999; Schmitt et al., 2002b). For numeric karyotypic analysis, at least twelve DAPI stained metaphases were counted per lymphoma sample (Schmitt et al., 2002b). Cytospin preparations of suspension cultures for subsequent SA-β-gal analyses or immunostainings, quantification of ROS by 2′-7′-dichlordihydrofluorescein-based flow cytometric analyses, and quantification of DNA strand breaks in Annexin V-negative cells (Miltenyi) by the Comet assay were carried out as previously described (Braig et al., 2005; Reimann et al., 2007). Detection of apoptotic DNA strand breaks by TUNEL (Roche) staining in paraffin-embedded tissue sections and assessment of SA-β-gal activity at pH 5.5 in cryosections or cytospin preparations of cell suspensions were carried out as described (Schmitt et al., 2002a; Schmitt et al., 1999).

Gene Expression Analysis

Genome-wide expression analysis was performed on RNA isolated with Trizol (Invitrogen) from whole lymph nodes derived from individual lymphoma-bearing mice and from normal spleen as control, or, in a second set of experiments, from short-term cultured lymphoma cells with and without exposure to 100 pM of human TGF-β1 for 24 hours using a 22.5 K mouse cDNA array. For RT-PCR analyses, RNA extracts were transcribed into cDNA using SuperScript reverse transcriptase (Invitrogen) and random hexamers or oligo-dT. Primer sequences and detailed PCR protocols for the detection of murine *ACE*, *Suv39h1*, *Suv39h2*, *TβRII-ED*, and *TATA box binding protein* (*TBP*; as an internal control) transcripts as well as for the RQ-PCR analyses of mouse *CIP1*, *CTGF*, *CXCL1*, *CXCL7*, *CXCL16*, *GAPDH*, *GM-CSF*, *IGFBP6*, *IGFBP7*, *IL-1α*, *IL-6*, *IL-7*, *INK4b*, *MCP-4*, *MIP-3α*, *MMP2*, *MMP3*, *Tgfig*, *TGF-β1*, *TGF-β2*, *TGF-β3*, and *VEGF* transcripts (using commercially available primers; Applied Biosystems) are available upon request. For every given sample, ΔCt values were determined as the difference between the Ct value of a specific transcript and the Ct value of *GAPDH*, serving as the housekeeping

control mRNA, and relative transcript levels (e.g., treated versus untreated) were then produced based on $2^{(-\Delta\Delta Ct)}$ with $\Delta\Delta Ct = \Delta Ct_{treated} - \Delta Ct_{untreated}$.

Immunophenotyping by flow cytometry and antigen detection by immunofluorescence, immunohistochemistry, immunoblotting, and immunoprecipitation were carried out as described (Reimann et al., 2007; Schmitt et al., 2002a). A summary of the methods and the complete list of antibodies used can be found in the Supplemental Experimental Procedures. Staining intensities of Smad3-P or PAI-1 in situ were semiquantitatively assessed (− versus +, ++, or +++; converted into numeric values 0, 1, 2, or 3 to calculate a mean in some experiments [where a value of around 0.5 would translate into (+)]). TGF-β1 protein concentrations were also measured by enzyme-linked immunosorbent assay (Quantikine, R&D Systems) in HCl-activated cell-free culture supernatant in accordance with the manufacturer's protocol.

Statistical Evaluation

Tumor onset data reflecting the latency between birth and first-time palpability of enlarged lymph nodes were compared using the log-rank (Mantel-Cox) test. Curve fitting analysis was done by linear regression with R^2 as the coefficient of determination. The unpaired t-test was used to compare means and standard deviations (SD). All quantifications from staining reactions (e.g., immunostainings, TUNEL, or SA-β-gal assays) were carried out by an independent and blinded second examiner, and reflect at least three samples with at least 200 events counted (typically in more than three different tissue areas) each.

ACCESSION NUMBERS

Details about the cDNA microarray protocols, the specific array design, and the respective data can be found at http://www.ebi.ac.uk/arrayexpress/ under accession number E-MEXP-1423 for the first set and E-MEXP-1424 for the second set of experiments.

SUPPLEMENTAL INFORMATION

Supplemental Information includes Supplemental Experimental Procedures and four figures and can be found with this article online at doi:10.1016/j.ccr.2009.12.043.

ACKNOWLEDGMENTS

We thank C. Barlow, M. Eilers, G. Evan, B. Falini, the late A. Harris, T. Jacks, P. Krimpenfort, P. Leder, A. Leutz, J. Massagué, J. Sherr, and L. Varesio for mice, cells, and materials; A. Lude, S. Maßwig, N. Mikuda, I. Nehlmeier, M. Schmock, and S. Spieckermann for technical assistance; and members of the Schmitt lab for discussions and editorial advice. This work was supported by a PhD fellowship to J.R.D. from the Boehringer Ingelheim Foundation, and grants to C.A.S. from the European Union, the Deutsche Forschungsgemeinschaft (KFO105 and TRR54), and the Deutsche Krebshilfe.

Received: August 3, 2009
Revised: November 27, 2009
Accepted: December 31, 2009
Published: March 15, 2010

REFERENCES

Acosta, J.C., O'Loghlen, A., Banito, A., Guijarro, M.V., Augert, A., Raguz, S., Fumagalli, M., Da Costa, M., Brown, C., Popov, N., et al. (2008). Chemokine signaling via the CXCR2 receptor reinforces senescence. Cell *133*, 1006–1018.

Adams, J.M., Harris, A.W., Pinkert, C.A., Corcoran, L.M., Alexander, W.S., Cory, S., Palmiter, R.D., and Brinster, R.L. (1985). The c-myc oncogene driven by immunoglobulin enhancers induces lymphoid malignancy in transgenic mice. Nature *318*, 533–538.

Aichele, P., Zinke, J., Grode, L., Schwendener, R.A., Kaufmann, S.H., and Seiler, P. (2003). Macrophages of the splenic marginal zone are essential for trapping of blood-borne particulate antigen but dispensable for induction of specific T cell responses. J. Immunol. *171*, 1148–1155.

Barlow, C., Hirotsune, S., Paylor, R., Liyanage, M., Eckhaus, M., Collins, F., Shiloh, Y., Crawley, J.N., Ried, T., Tagle, D., and Wynshaw-Boris, A. (1996). Atm-deficient mice: a paradigm of ataxia telangiectasia. Cell *86*, 159–171.

Bartkova, J., Rezaei, N., Liontos, M., Karakaidos, P., Kletsas, D., Issaeva, N., Vassiliou, L.V., Kolettas, E., Niforou, K., Zoumpourlis, V.C., et al. (2006). Oncogene-induced senescence is part of the tumorigenesis barrier imposed by DNA damage checkpoints. Nature *444*, 633–637.

Braig, M., Lee, S., Loddenkemper, C., Rudolph, C., Peters, A.H., Schlegelberger, B., Stein, H., Dorken, B., Jenuwein, T., and Schmitt, C.A. (2005). Oncogene-induced senescence as an initial barrier in lymphoma development. Nature *436*, 660–665.

Campisi, J., and d'Adda di Fagagna, F. (2007). Cellular senescence: when bad things happen to good cells. Nat. Rev. Mol. Cell Biol. *8*, 729–740.

Christophorou, M.A., Martin-Zanca, D., Soucek, L., Lawlor, E.R., Brown-Swigart, L., Verschuren, E.W., and Evan, G.I. (2005). Temporal dissection of p53 function in vitro and in vivo. Nat. Genet. *37*, 718–726.

Collado, M., Gil, J., Efeyan, A., Guerra, C., Schuhmacher, A.J., Barradas, M., Benguria, A., Zaballos, A., Flores, J.M., Barbacid, M., et al. (2005). Tumour biology: senescence in premalignant tumours. Nature *436*, 642.

Coppe, J.P., Patil, C.K., Rodier, F., Sun, Y., Munoz, D.P., Goldstein, J., Nelson, P.S., Desprez, P.Y., and Campisi, J. (2008). Senescence-associated secretory phenotypes reveal cell-nonautonomous functions of oncogenic RAS and the p53 tumor suppressor. PLoS Biol. *6*, 2853–2868.

Cordenonsi, M., Dupont, S., Maretto, S., Insinga, A., Imbriano, C., and Piccolo, S. (2003). Links between tumor suppressors: p53 is required for TGF-beta gene responses by cooperating with Smads. Cell *113*, 301–314.

Courtois-Cox, S., Genther Williams, S.M., Reczek, E.E., Johnson, B.W., McGillicuddy, L.T., Johannessen, C.M., Hollstein, P.E., MacCollin, M., and Cichowski, K. (2006). A negative feedback signaling network underlies oncogene-induced senescence. Cancer Cell *10*, 459–472.

Dave, S.S., Wright, G., Tan, B., Rosenwald, A., Gascoyne, R.D., Chan, W.C., Fisher, R.I., Braziel, R.M., Rimsza, L.M., Grogan, T.M., et al. (2004). Prediction of survival in follicular lymphoma based on molecular features of tumor-infiltrating immune cells. N. Engl. J. Med. *351*, 2159–2169.

Davies, J.Q., and Gordon, S. (2005). Isolation and culture of human macrophages. Methods Mol. Biol. *290*, 105–116.

Deng, C., Zhang, P., Harper, J.W., Elledge, S.J., and Leder, P. (1995). Mice lacking p21CIP1/WAF1 undergo normal development, but are defective in G1 checkpoint control. Cell *82*, 675–684.

Di Micco, R., Fumagalli, M., Cicalese, A., Piccinin, S., Gasparini, P., Luise, C., Schurra, C., Garre, M., Nuciforo, P.G., Bensimon, A., et al. (2006). Oncogene-induced senescence is a DNA damage response triggered by DNA hyper-replication. Nature *444*, 638–642.

Dimri, G.P., Lee, X., Basile, G., Acosta, M., Scott, G., Roskelley, C., Medrano, E.E., Linskens, M., Rubelj, I., Pereira-Smith, O., et al. (1995). A biomarker that identifies senescent human cells in culture and in aging skin in vivo. Proc. Natl. Acad. Sci. USA *92*, 9363–9367.

Dokmanovic, M., Chang, B.D., Fang, J., and Roninson, I.B. (2002). Retinoid-induced growth arrest of breast carcinoma cells involves co-activation of multiple growth-inhibitory genes. Cancer Biol. Ther. *1*, 24–27.

Egle, A., Harris, A.W., Bouillet, P., and Cory, S. (2004). Bim is a suppressor of Myc-induced mouse B cell leukemia. Proc. Natl. Acad. Sci. USA *101*, 6164–6169.

Evan, G.I., Wyllie, A.H., Gilbert, C.S., Littlewood, T.D., Land, H., Brooks, M., Waters, C.M., Penn, L.Z., and Hancock, D.C. (1992). Induction of apoptosis in fibroblasts by c-myc protein. Cell *69*, 119–128.

Feldser, D.M., and Greider, C.W. (2007). Short telomeres limit tumor progression in vivo by inducing senescence. Cancer Cell *11*, 461–469.

Grandori, C., Wu, K.J., Fernandez, P., Ngouenet, C., Grim, J., Clurman, B.E., Moser, M.J., Oshima, J., Russell, D.W., Swisshelm, K., et al. (2003). Werner syndrome protein limits MYC-induced cellular senescence. Genes Dev. *17*, 1569–1574.

Guney, I., Wu, S., and Sedivy, J.M. (2006). Reduced c-Myc signaling triggers telomere-independent senescence by regulating Bmi-1 and p16(INK4a). Proc. Natl. Acad. Sci. USA *103*, 3645–3650.

Hans, C.P., Weisenburger, D.D., Greiner, T.C., Gascoyne, R.D., Delabie, J., Ott, G., Muller-Hermelink, H.K., Campo, E., Braziel, R.M., Jaffe, E.S., et al. (2004). Confirmation of the molecular classification of diffuse large B-cell lymphoma by immunohistochemistry using a tissue microarray. Blood *103*, 275–282.

Hemann, M.T., and Narita, M. (2007). Oncogenes and senescence: breaking down in the fast lane. Genes Dev. *21*, 1–5.

Huynh, M.L., Fadok, V.A., and Henson, P.M. (2002). Phosphatidylserine-dependent ingestion of apoptotic cells promotes TGF-beta1 secretion and the resolution of inflammation. J. Clin. Invest. *109*, 41–50.

Jacks, T., Remington, L., Williams, B.O., Schmitt, E.M., Halachmi, S., Bronson, R.T., and Weinberg, R.A. (1994). Tumor spectrum analysis in p53-mutant mice. Curr. Biol. *4*, 1–7.

Kamijo, T., Zindy, F., Roussel, M.F., Quelle, D.E., Downing, J.R., Ashmun, R.A., Grosveld, G., and Sherr, C.J. (1997). Tumor suppression at the mouse INK4a locus mediated by the alternative reading frame product p19ARF. Cell *91*, 649–659.

Krimpenfort, P., Quon, K.C., Mooi, W.J., Loonstra, A., and Berns, A. (2001). Loss of p16Ink4a confers susceptibility to metastatic melanoma in mice. Nature *413*, 83–86.

Kuilman, T., Michaloglou, C., Vredeveld, L.C., Douma, S., van Doorn, R., Desmet, C.J., Aarden, L.A., Mooi, W.J., and Peeper, D.S. (2008). Oncogene-induced senescence relayed by an interleukin-dependent inflammatory network. Cell *133*, 1019–1031.

Lachner, M., O'Carroll, D., Rea, S., Mechtler, K., and Jenuwein, T. (2001). Methylation of histone H3 lysine 9 creates a binding site for HP1 proteins. Nature *410*, 116–120.

Laiho, M., DeCaprio, J.A., Ludlow, J.W., Livingston, D.M., and Massague, J. (1990). Growth inhibition by TGF-beta linked to suppression of retinoblastoma protein phosphorylation. Cell *62*, 175–185.

Lauber, K., Bohn, E., Krober, S.M., Xiao, Y.J., Blumenthal, S.G., Lindemann, R.K., Marini, P., Wiedig, C., Zobywalski, A., Baksh, S., et al. (2003). Apoptotic cells induce migration of phagocytes via caspase-3-mediated release of a lipid attraction signal. Cell *113*, 717–730.

Lee, A.C., Fenster, B.E., Ito, H., Takeda, K., Bae, N.S., Hirai, T., Yu, Z.X., Ferrans, V.J., Howard, B.H., and Finkel, T. (1999). Ras proteins induce senescence by altering the intracellular levels of reactive oxygen species. J. Biol. Chem. *274*, 7936–7940.

Lenz, G., Wright, G., Dave, S.S., Xiao, W., Powell, J., Zhao, H., Xu, W., Tan, B., Goldschmidt, N., Iqbal, J., et al. (2008). Stromal gene signatures in large-B-cell lymphomas. N. Engl. J. Med. *359*, 2313–2323.

Lin, H.K., Bergmann, S., and Pandolfi, P.P. (2004). Cytoplasmic PML function in TGF-beta signalling. Nature *431*, 205–211.

Mallette, F.A., Gaumont-Leclerc, M.F., and Ferbeyre, G. (2007). The DNA damage signaling pathway is a critical mediator of oncogene-induced senescence. Genes Dev. *21*, 43–48.

Martins, C.P., Brown-Swigart, L., and Evan, G.I. (2006). Modeling the therapeutic efficacy of p53 restoration in tumors. Cell *127*, 1323–1334.

Michaloglou, C., Vredeveld, L.C., Soengas, M.S., Denoyelle, C., Kuilman, T., van der Horst, C.M., Majoor, D.M., Shay, J.W., Mooi, W.J., and Peeper, D.S. (2005). BRAFE600-associated senescence-like cell cycle arrest of human naevi. Nature *436*, 720–724.

Narita, M., Nunez, S., Heard, E., Lin, A.W., Hearn, S.A., Spector, D.L., Hannon, G.J., and Lowe, S.W. (2003). Rb-mediated heterochromatin formation and silencing of E2F target genes during cellular senescence. Cell *113*, 703–716.

Peters, A.H., O'Carroll, D., Scherthan, H., Mechtler, K., Sauer, S., Schofer, C., Weipoltshammer, K., Pagani, M., Lachner, M., Kohlmaier, A., et al. (2001). Loss of the Suv39h histone methyltransferases impairs mammalian heterochromatin and genome stability. Cell *107*, 323–337.

Reimann, M., Loddenkemper, C., Rudolph, C., Schildhauer, I., Teichmann, B., Stein, H., Schlegelberger, B., Dorken, B., and Schmitt, C.A. (2007). The Myc-evoked DNA damage response accounts for treatment resistance in primary lymphomas in vivo. Blood *110*, 2996–3004.

Savill, J., and Fadok, V. (2000). Corpse clearance defines the meaning of cell death. Nature *407*, 784–788.

Schmitt, C.A., McCurrach, M.E., de Stanchina, E., Wallace-Brodeur, R.R., and Lowe, S.W. (1999). INK4a/ARF mutations accelerate lymphomagenesis and promote chemoresistance by disabling p53. Genes Dev. *13*, 2670–2677.

Schmitt, C.A., Rosenthal, C.T., and Lowe, S.W. (2000). Genetic analysis of chemoresistance in primary murine lymphomas. Nat. Med. *6*, 1029–1035.

Schmitt, C.A., Fridman, J.S., Yang, M., Lee, S., Baranov, E., Hoffman, R.M., and Lowe, S.W. (2002a). A senescence program controlled by p53 and p16INK4a contributes to the outcome of cancer therapy. Cell *109*, 335–346.

Schmitt, C.A., Yang, M., Fridman, J.S., Baranov, E., Hoffman, R.M., and Lowe, S.W. (2002b). Dissecting p53 tumor suppressor functions in vivo. Cancer Cell *1*, 289–298.

Schwarz, J.K., Bassing, C.H., Kovesdi, I., Datto, M.B., Blazing, M., George, S., Wang, X.F., and Nevins, J.R. (1995). Expression of the E2F1 transcription factor overcomes type beta transforming growth factor-mediated growth suppression. Proc. Natl. Acad. Sci. USA *92*, 483–487.

Seoane, J., Le, H.V., and Massague, J. (2002). Myc suppression of the p21(Cip1) Cdk inhibitor influences the outcome of the p53 response to DNA damage. Nature *419*, 729–734.

Serrano, M., Lin, A.W., McCurrach, M.E., Beach, D., and Lowe, S.W. (1997). Oncogenic ras provokes premature cell senescence associated with accumulation of p53 and p16INK4a. Cell *88*, 593–602.

Spender, L.C., and Inman, G.J. (2009). TGF-beta induces growth arrest in Burkitt lymphoma cells via transcriptional repression of E2F-1. J. Biol. Chem. *284*, 1435–1442.

Strasser, A., Harris, A.W., Bath, M.L., and Cory, S. (1990). Novel primitive lymphoid tumours induced in transgenic mice by cooperation between myc and bcl-2. Nature *348*, 331–333.

Thomas, D.A., and Massague, J. (2005). TGF-beta directly targets cytotoxic T cell functions during tumor evasion of immune surveillance. Cancer Cell *8*, 369–380.

Vafa, O., Wade, M., Kern, S., Beeche, M., Pandita, T.K., Hampton, G.M., and Wahl, G.M. (2002). c-Myc can induce DNA damage, increase reactive oxygen species, and mitigate p53 function: a mechanism for oncogene-induced genetic instability. Mol. Cell *9*, 1031–1044.

Wajapeyee, N., Serra, R.W., Zhu, X., Mahalingam, M., and Green, M.R. (2008). Oncogenic BRAF induces senescence and apoptosis through pathways mediated by the secreted protein IGFBP7. Cell *132*, 363–374.

Xue, W., Zender, L., Miething, C., Dickins, R.A., Hernando, E., Krizhanovsky, V., Cordon-Cardo, C., and Lowe, S.W. (2007). Senescence and tumour clearance is triggered by p53 restoration in murine liver carcinomas. Nature *445*, 656–660.